

Tailoring microstructure and properties of Ti-6Al-4V from piston-based material extrusion through hot isostatic pressing

Powder Metallurgy
1–6

© The Author(s) 2026



Article reuse guidelines:

sagepub.com/journals-permissions

DOI: 10.1177/00325899261454936

journals.sagepub.com/home/pmg



Katharina Bartsch¹, Dirk Herzog^{1,2} , Lennart Waalkes¹ , Kevin Janzen¹ , Stefan Grottker¹, Sebastian Mansky¹ , Ingomar Kelbassa^{1,2} , Roman Schöneich², James Shipley³ and Johannes Gårdstam³

Abstract

Piston-based material extrusion (PEX) is an additive manufacturing technology that enables the processing of metal injection moulding (MIM) feedstock to form green parts. The extrusion process does not require moulds and hence is a competitive alternative for the shaping of MIM process routes, offering short lead times and cost-efficiency for lower lot sizes, while integrating into the remaining process chain and equipment. This paper focuses on the microstructure and properties of Ti-6Al-4V fabricated by PEX and followed by a subsequent hot isostatic pressing (HIP) step for parts requiring superior density and mechanical properties. The HIP process is performed using standard as well as high-purity conditions (Quintus Purus[®]). After sintering, a globular, mostly α microstructure is observed. A subsequent HIP followed by rapid quenching transforms the microstructure to a bi-modal state. A similar effect on microstructure is observed for the Quintus Purus[®] HIP; however, the formation of α -case on the part surface is avoided. While the mean density of the sintered parts is 97.2%, HIP leads to an increase to 98.9–99.3% with the remnant porosity mainly stemming from open, connected pores. Although the sintered specimens already fulfil the industrial requirements, the Quintus Purus[®] HIP leads to a slight increase in yield and ultimate tensile strength at minimal reduction of elongation. The standard HIP shows the same but slightly more pronounced trend. The results show that by a careful design of the specific HIP conditions, the microstructure and properties can be tailored for a specific application.

Keywords

additive manufacturing, hot isostatic pressing, titanium alloy, piston-based material extrusion, microstructure, mechanical properties

Received: 22 July 2025; accepted: 29 April 2026

Introduction

Metal injection moulding (MIM) is a well-known production technology where metal powders and polymer binders are combined to a feedstock which is moulded to a green part, debound and sintered.¹ Due to the injection process, a mould is required, which is economically feasible at high quantities only.² Correspondingly, the development of additive manufacturing (AM) technologies using the same feedstock as the MIM process is of high interest to enable the manufacturing of functional prototypes, custom-made or complex structures within the same production line. Three different approaches to processing MIM feedstock via AM have been developed^{3,4}: fused filament fabrication (FFF), fused granular fabrication (FGF), and piston-based material extrusion (PEX). Adapted from the polymer-based material extrusion AM process, also commonly known as fused deposition modelling, the FFF technology utilises a metal filament. Compared to the MIM feedstock, changes to the binder system are often necessary to, for example, account for the required flexibility of the filament to allow for spooling by adding elastomers⁵ or amorphous polyolefins.⁶ These changes may have a great impact on the subsequent steps

of debinding and sintering. Hence, AM technologies capable of directly processing the MIM feedstock are preferable.⁴ FGF is characterised as a screw-based extrusion process where the granular feedstock is extruded by a screw mounted on one of the AM system's axes. FGF is capable of using the MIM feedstock^{7,8} and offers continuous and fast material feed rates.⁹ However, FGF struggles with process stability.¹⁰ Furthermore, the complex screw setup increases the machine costs,¹¹ reducing the cost advantage of AM over MIM. To address the main disadvantages of FFF and FGF, PEX setups have been developed. Here, a piston enables the extrusion of the MIM feedstock rather than a screw.¹² The use of a piston simplifies the printing unit significantly, thus decreasing the

¹Fraunhofer IAPT, Hamburg, Germany

²Hamburg University of Technology, Institute for Industrialization of Smart Materials, Hamburg, Germany

³Quintus Technologies AB, Västerås, Sweden

Corresponding author:

Kevin Janzen, Fraunhofer IAPT, Am Schleusenengraben 14, 21029 Hamburg, Germany.

Email: kevin.janzen@iapt.fraunhofer.de

machine cost. Different from FGF, PEX is not able to continuously extrude material since the process stops as soon as the filling quantity of the piston is discharged.⁹

To enable the seamless integration of PEX in MIM production, the properties of the respective green parts must be similar. Therefore, the PEX process design must be chosen carefully to avoid under-extrusion.⁴ The resulting rhomboid voids between adjacent extrusion paths reduce the density of the green part and remain in the sintered part, leading to decreased mechanical properties. Apart from the increased porosity, delamination of consecutive layers can take place, which is a well-known and characteristic defect for AM parts in general.

Given an appropriate process design, the properties of the sintered PEX part are comparable to MIM parts, including the typical defects such as cracks initiated from closed pores or sinter porosity. Density of the sintered part is in accordance with ASTM F2885-11 (>96%) with usually >98%. Tensile properties are also met. However, the layer-wise nature of AM leads to anisotropic behaviour regarding shrinkage and tensile properties.^{4,13}

For sintered parts requiring superior density and tensile properties, hot isostatic pressing (HIP) is a suitable post-processing approach¹⁴ with increasing application in the metal AM field.^{15,16} In HIP, a defined combination of temperature and pressure is applied for a set period of time. The temperature is set to allow for plastic flow. Correspondingly, the applied pressure results in a substantial shrinkage of any closed pore to a size not detectable by typical analysis technologies such as scanning electron microscopy.¹⁵ Open porosity may only be reduced by encapsulation or coating.¹⁷ However, metal parts with a density > 90–95% are known to feature mainly closed pores and thus can be completely compacted,¹⁸ which indicates the feasibility of HIP application to PEX parts to improve mechanical properties.

In this study, the influence of HIP application to Ti-6Al-4V sintered PEX parts is investigated. A standard HIP treatment, as well as high-purity conditions (Quintus Purus[®]) with regard to the furnace atmosphere, are compared to the as-sintered state of the material. Changes to the microstructure as well as the mechanical properties are evaluated and discussed.

Methods and materials

To investigate the influence of HIP treatments on PEX parts, the following experimental setup is used.

Specimen manufacture

Cubes with the dimension of $10 \times 10 \times 10 \text{ mm}^3$ are chosen as specimen geometry to avoid any influence of geometric features. The titanium alloy Ti-6Al-4V (6.14% Al and 4.06% Vanadium) with a particle size distribution of $D_{90} = 23 \mu\text{m}$ is used as it is a common material in MIM. The PEX system, similar to the one given by Waalkes et al.,⁴ is employed for the manufacturing. The process parameters are given in Table 1. To be able to identify limits of the HIP treatment, the print speed is chosen as double the maximum feasible print speed determined by Waalkes et al.⁴ to provoke defects

Table 1. Printing parameters for PEX manufacturing of the specimen.

Parameter	Value
Print speed	16 mm/s
Nozzle temperature	140 °C
Bed temperature	60 °C
Layer height	0.2 mm
Track width	0.45 mm

within the green part. A total of 12 specimens is manufactured, 4 specimens each for the as-sintered, standard HIP and Quintus Purus[®] HIP conditions.

Debinding and sintering of the green parts is performed by the service provider Element22 GmbH (Kiel, Germany). As this is an industrially used process chain, only some of the process parameters have been published.¹⁹ At the beginning, solvent debinding takes place using hexane at 40 °C for 18 h. The components are then placed in an integrated debinding and sintering furnace, in which the remaining binder components are thermally removed. The final sintering step takes place in a high vacuum ($\leq 10^{-3}$ mbar) at a temperature below or around the β -transus temperature (max. 1100 °C) for less than 5 h to avoid coarsening of the microstructure and preserve the superior mechanical properties of the fine-grained microstructure.

HIP treatment

The HIP treatments follow the same scheme of temperature and pressure application, actual treatment and cooling phase. In the standard HIP treatment, temperature and pressure are linearly increased to 100 MPa and 920 °C over the period of 1 h and held at that level for 2 h. Finally, the pressure is released over a period of 20 min, and cooling takes place simultaneously. The Quintus Purus[®] HIP treatment is initiated with a preheating sequence of 1 h. Afterwards, the temperature and pressure are linearly increased to 920 °C and 100 MPa, respectively. The pressure release and cooling only take 10 min compared to the standard HIP procedure.

Specimen preparation and evaluation

All cubes are prepared for the measurements according to DIN EN ISO 4499-1. The relative density of the specimens is evaluated optically using a digital microscope (VHX-5000, KEYENCE DEUTSCHLAND GmbH, Neu-Isenberg, Germany). For microstructure evaluation, the prepared surface is etched and also subjected to the digital microscope. To determine the local mechanical properties of the specimens, the i3D[®] technology of Imprintec GmbH (Bochum, Germany) is applied. Here, the material pile-up of local indentations on the specimen's surface is optically measured and analysed with regard to various mechanical properties such as yield strength, ultimate tensile strength and elongation at failure. As the measurement directly on the as-sintered/as-HIP surface proved unreliable because of the surface roughness, the specimens are embedded in resin and ground using an 80-grit grinding disk. Figure 1 shows the prepared specimens (left) as well as the positioning of

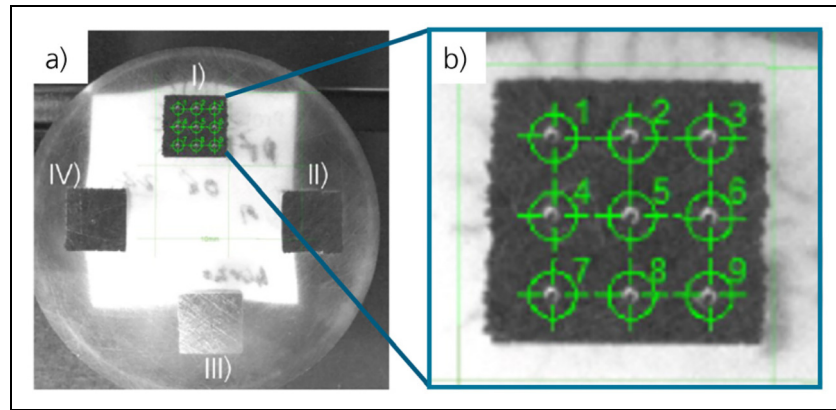


Figure 1. Cubic specimen (a) and corresponding indentation points (b).

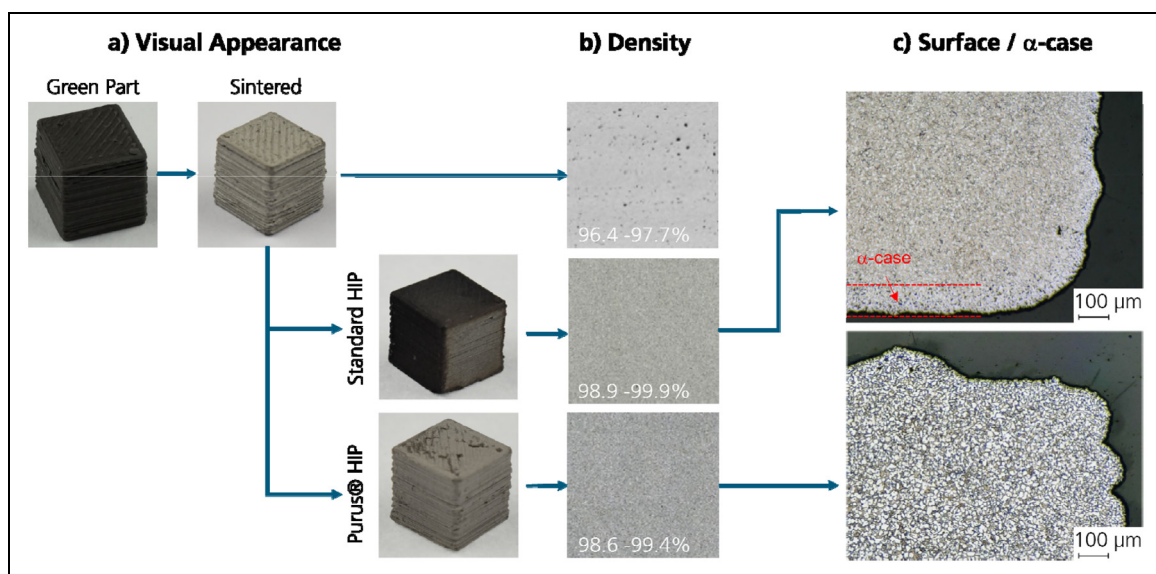


Figure 2. Cubic specimens in as-built, sintered and HIPed state (a), resulting density values (b), and observed α -case on surface of standard-HIPed samples (c).

the indentation points on a specimen's surface. With 9 indentation points per cube, a total of 108 data points have been created and analysed. Eleven data points were identified as outliers and therefore excluded from further evaluation.

Results and discussion

Density

The as-printed specimens reach density values between 96.4% and 97.7% after sintering, with a mean density of 97.2%, cf. Figure 2. The appearance of the sintered specimens is mostly metallic, showing no coloration.

After the standard HIP treatment, the specimens show a mostly oxidic surface. Microscopic investigations confirm the presence of surface oxidation and resulting α -case (cf. Figure 2(c)). The density is increased to a mean value of 99.3%, with remaining porosity originating from delaminated sections and thus open porosity.

Using the Quintus Purus® HIP process, specimens remain in a mostly metallic appearance and do not show pronounced signs of oxidation on the surface. No α -casing is observed on

the samples. The mean density of the specimens subjected to Quintus Purus® HIP is found to be 98.9%. Again, the remaining porosity appears to be originating from delaminated sections. Differences in density between standard and Quintus Purus® HIP procedure are therefore mainly attributed to fluctuations in quality of the ingoing, sintered PEX specimens rather than other possible influences, for example, oxygen uptake.

Microstructure

The sintered specimens show a fine-grained and globular, mostly α microstructure, similar to the one reported by Waalkes et al.⁴ using the identical sintering procedure (Figure 3(a) and (e)). After the sub- β -transus standard HIP, the resulting microstructure is bi-modal (Figure 3(b)) with fine acicular grains and retained α -grains from the ingoing sintered microstructure (cf. detail in Figure 3(e)). A comparable microstructure results from the Quintus Purus® HIP treatment (Figure 3(c)). In the detail shown in Figure 3(f), the retained α -grains appear to be slightly larger. As the only difference in the two HIP cycles is the purer

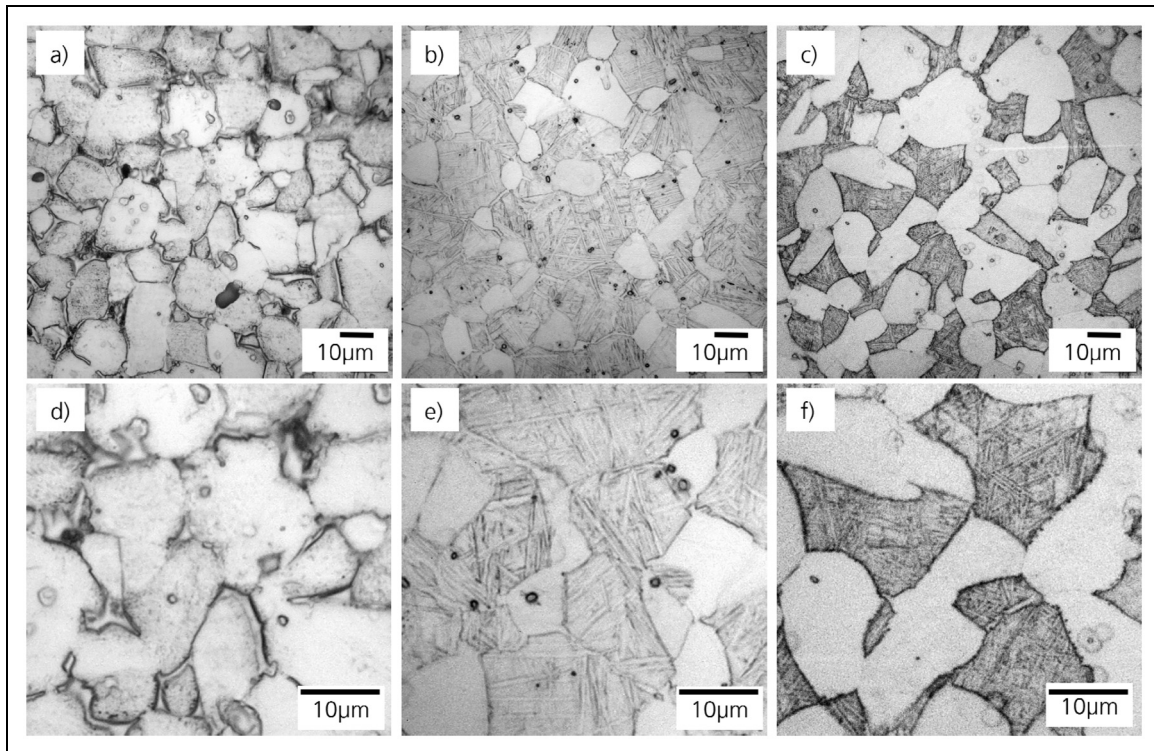


Figure 3. Overview (a–c) and detail (d–f) of microstructure of sintered (a, d), standard HIP (b, e), and Quintus Purus[®] HIP (c, f) specimens.

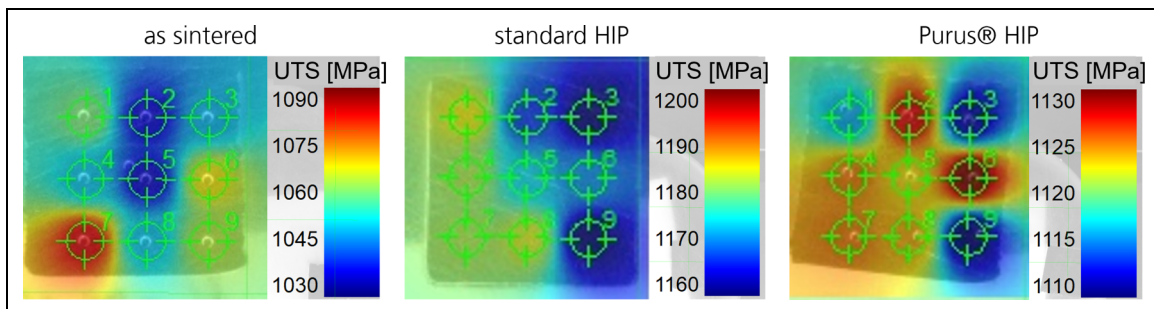


Figure 4. Local values obtained for UTS on sintered (left), standard HIP (centre), and Quintus Purus[®] HIP (right) specimens.

atmosphere, this could be attributed to a lower presence of oxygen in the vessel.

Local mechanical properties

Using the indentation method as discussed in section ‘Methods and materials’, all samples are tested for their local properties. Representative measurements for each condition are given in Figure 4. Please note the different scales when comparing between specimens.

The mechanical properties are evaluated with regard to the yield strength (YS), ultimate tensile strength (UTS), and elongation at break (A) depending on the condition, that is, as sintered, standard HIP and Quintus Purus[®] HIP (cf. Figure 5). No local pattern is observed within the position of the individual indentation points, which is plausible considering the simple and rather small cube geometry. Thus, mean values are calculated for each individual specimen over all valid indentation points. Further, the mean values for a condition are then generated by the mean values of

the specimens. In Figure 5, the overall mean values per condition and the mean values obtained on the specimen showing the lowest performance are displayed in addition to the lowest individual measurement point (i.e. originating from a single indentation).

Both HIP procedures show a strengthening effect while slightly reducing the elongation. This effect is more pronounced in the standard HIP samples compared to the Quintus Purus[®] HIP samples. Possible explanations include either a higher oxygen uptake during the standard HIP procedure or differences originating from slight temperature and cooling rate variations.

The mechanical properties of all specimens meet the requirements of both standards, ASTM F2885 and ISO 22068.

Conclusion

The HIP of specimens originating from PEX successfully increased the density. Due to the PEX processing parameters

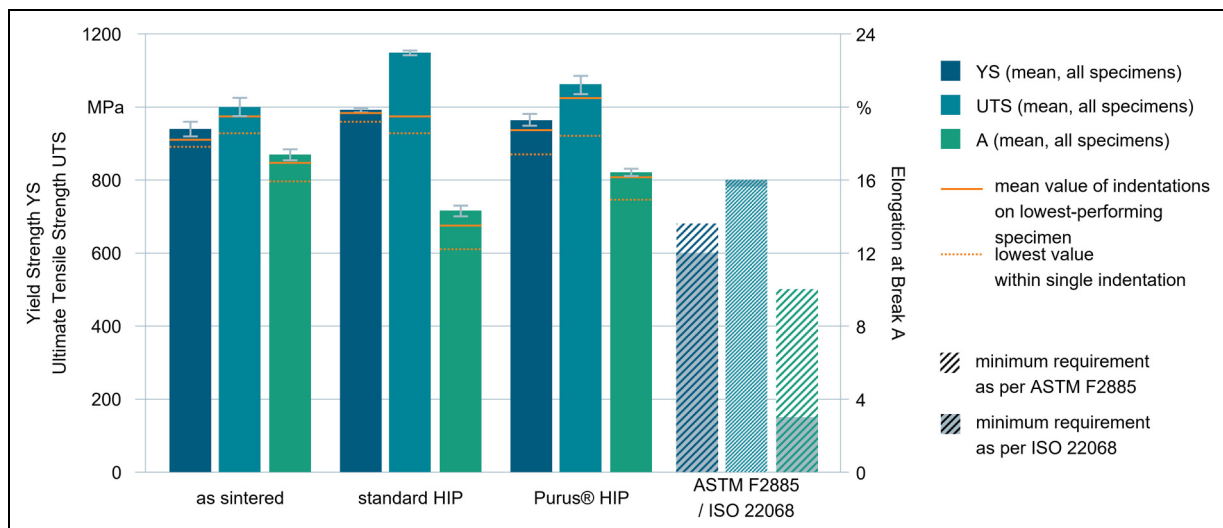


Figure 5. Mechanical properties obtained on the as-sintered, standard HIP and Quintus Purus[®] HIP specimens, and comparison with ASTM F2885 and ISO 22068 requirements.

used in this study, as-sintered cubes showed considerable variation in densities among specimens, with some connected porosity. The slight density differences observed between standard- and Quintus Purus[®] HIP are therefore not necessarily related to the HIP conditions, as HIP is known to be effective on closed porosity only. Both HIP variants transform the microstructure from mostly α to bimodal, with Quintus Purus[®] HIP appearing to retain slightly more of the ingoing α -grains from the as-sintered state. The Quintus Purus[®] HIP condition successfully avoids the formation of α -case.

Using the indentation method, it was possible to locally identify the mechanical properties of the PEX specimens. No significant variation of the local properties over the cubic samples was found. Mechanical properties of the as-sintered specimens already fulfil ASTM F2885 and ISO 22068 requirements; however, HIP shows the potential to tailor strength and elongation to the exact needs of an application, safely within the above-mentioned standards. Standard HIP leads to the greatest improvement in mean strength values (YS: +53 MPa, UTS: +146 MPa), while reducing elongation (A: -3.41%-pts). Quintus Purus[®] HIP leads to more moderate strength and elongation changes (YS: +24 MPa, UTS: +60 MPa, A: -0.96%-pts). In addition, HIP adds an extra safety margin to density requirements, as long as closed porosity is concerned.

Further investigations are needed to identify the exact causes for the slight variation of the mechanical properties obtained when comparing the standard and Quintus Purus[®] HIP procedure. Also, as fatigue properties are known to be improved by HIP treatments, possible differences in the effect of standard and Quintus Purus[®] HIP on the fatigue properties are subject to further research.

Acknowledgements

Part of this work was carried out within the joint project AMProSint (02P20K044), which was funded by the Federal Ministry of Education and Research (BMBF) in the ‘Innovations for the production, services and work of tomorrow’ program and supervised by the

Project Management Agency Karlsruhe (PTKA). The authors would like to express their gratitude for the funding. The authors would also like to thank Element22 GmbH (Kiel, Germany) for performing the sintering step within their production line.

ORCID iDs

Dirk Herzog <https://orcid.org/0000-0001-7059-6151>
 Kevin Janzen <https://orcid.org/0000-0002-3932-4788>
 Sebastian Mansky <https://orcid.org/0009-0005-7385-6939>
 Ingomar Kelbassa <https://orcid.org/0009-0003-1325-4472>

Funding

The authors disclosed receipt of the following financial support for the research, authorship, and/or publication of this article: This work was supported by the Bundesministerium für Bildung und Forschung (grant number AMProSint (02P20K044)).

Declaration of conflicting interests

The authors declared no potential conflicts of interest with respect to the research, authorship, and/or publication of this article.

References

- German RM and Bose A. Injection molding of metals and ceramics. *Powder Metall* 1997; 42: 157–160.
- German RM. Metal powder injection molding (MIM): key trends and markets. In: *Handbook of metal injection molding*. Netherlands: Elsevier, 2019, pp.1–21.
- Gonzalez-Gutierrez J, Cano S, Schuschnigg S, et al. Additive manufacturing of metallic and ceramic components by the material extrusion of highly-filled polymers: a review and future perspectives. *Materials* 2018; 11: 840.
- Waalkes L, Längerich J, Imgrund P, et al. Piston-based material extrusion of Ti-6Al-4V feedstock for complementary use in metal injection molding. *Materials* 2022; 15: 51.
- Danforth SC, Agarwala MK, Bandyopadhyay A, et al. *Solid freeform fabrication methods*. U.S. Patent US5900207A, 1999.

6. McNulty TF, Mohammadi F, Bandyopadhyay A, et al. Development of a binder formulation for fused deposition of ceramics. *Rapid Prototyp J* 1998; 4: 144–150.
7. Singh G, Missiaen J-M, Bouvard D, et al. Copper extrusion 3D printing using metal injection moulding feedstock: analysis of process parameters for green density and surface roughness optimization. *Addit Manuf* 2021; 38: 101778.
8. Singh G, Missiaen J-M, Bouvard D, et al. Additive manufacturing of 17-4 PH steel using metal injection molding feedstock: analysis of 3D extrusion printing, debinding and sintering. *Addit Manuf* 2021; 47: 102287.
9. Waalkes L, Längerich J, Holbe F, et al. Feasibility study on piston-based feedstock fabrication with Ti-6Al-4V metal injection molding feedstock. *Addit Manuf* 2020; 35: 101207.
10. Bellini A, Shor L and Guceru SI. New developments in fused deposition modeling of ceramics. *Rapid Prototyp J* 2005; 11: 214–220.
11. Valkenaers H, Vogeler F, Ferraris E, et al. A novel approach to additive manufacturing: screw extrusion 3D-printing. In: Proceedings of the 10th international conference on multi-material micro manufacture, Singapore, 2013, pp.235–238.
12. Greul M, Staskewitsch E, Steger W, et al. *Process and apparatus for the free-forming manufacture of three dimensional components of pre-determined shape*. U.S. Patent US5649277A, 1997.
13. Lieberwirth C, Harder A and Seitz H. Extrusion based additive manufacturing of metal parts. *J Mech Eng Autom* 2017; 7: 79–83.
14. Loh NL and Sia KY. An overview of hot isostatic pressing. *J Mater Process Technol* 1992; 30: 45–65.
15. Herzog D, Bartsch K and Bossen B. Productivity optimization of laser powder bed fusion by hot isostatic pressing. *Addit Manuf* 2020; 36: 101494.
16. Qian M, Xu W, Brandt M, et al. Additive manufacturing and postprocessing of Ti-6Al-4V for superior mechanical properties. *MRS Bull* 2016; 41: 775–784. *Metallic Materials for 3D Printing*.
17. Atkinson HV and Davies S. Fundamental aspects of hot isostatic pressing: an overview. *Metall Mater Trans A* 2000; 31: 2981–3000.
18. Herrmann M and Raethel J. Hot pressing and hot isostatic pressing. In: Pomeroy M (eds) *Encyclopedia of materials: technical ceramics and glasses*. Amsterdam: Elsevier, 2021, pp.270–277.
19. Viehöfer U, Winkelmueller W, Lang M, et al. *Method for producing components from titanium or titanium alloys with powder metallurgy*. European Patent EP3231536A1, 2017.